



## Virtual Investigation of 'N' Heterocyclics for Treatment of Diabetes and Obesity

Harshada H. Puranik<sup>a</sup>, Asha B. Thomas<sup>a\*</sup>, Sohan S. Chitlange

<sup>a</sup>Dr. D. Y. Patil Institute of Pharmaceutical Sciences and Research, Pimpri,  
Pune, Maharashtra India

**\*Corresponding Author**

Dr. Asha B. Thomas

Department of Pharmaceutical Chemistry

Dr. D. Y. Patil Institute of Pharmaceutical Sciences and Research, Pimpri,  
Pune, Maharashtra India

---

### ABSTRACT:

Obesity and associated metabolic disorders became the global issue. Various treatment strategies have been employed for the comfort and recovery of the diseased condition. Patients suffering with obesity are many times found to be diabetic. Diacylglycerol o-acyl transferase inhibitor (DGAT<sub>i</sub>/ DGAT inhibitor) is found to be most effective treatment in management of diabetes mellitus, obesity and hyperlipidemia as well. Obesity causes the accumulation of triglycerides (TGs) in adipose tissue. The enzyme pancreatic lipase hydrolyzes the triglyceride to monoacylglycerol and fatty acids. DGAT is involved in catalysis of the very last step of triglyceride synthesis. DGAT-I is present in adipose tissue, liver and small intestine. DGAT-I plays a vital role in the absorption of lipid, also in accumulation of fat cells in the liver. Animal studies indicated that inhibition of this DGAT-I enzyme is a promising target for the treatment and management of obesity and diabetes mellitus and related metabolic disorders. The physicochemical properties, pharmacokinetics, drug-likeness, lead likeliness, synthetic accessibility of the newly designed ligands was investigated through computational screening. Biological activity was predicted using Molinspiration. The anti-diabetic potential of these ligands was predicted with PASS online (Prediction of Activity Spectra for Substances), and about 36 molecules were investigated through this process. The results obtained from this research work may be utilized for the development of new anti-diabetic, anti-obesity, anti-cancer

20264

drugs. Further these molecules must be explored to higher computational studies at molecular and cellular levels. In-vivo and in-vitro studies can also be performed to forecast the promising treatment strategy for diabetes mellitus and obesity.

**KEYWORDS:** DGAT-I inhibitors, anti-diabetic, anti-obesity, SwissADME, PASS online, Molinspiration

---

## **1. INTRODUCTION:**

Since the last decade, occurrence of type 2 Diabetes Mellitus (T2DM) has increased in huge numbers which is combined with cardiovascular diseases. Humans nowadays are particularly prone to obesity. Numerous notable advancements in the study of obesity have been made during the past few years. Triglycerides are believed to be the primary way that extra calories stored in fat [1]. The main characteristic of obesity is unusual deposits of fat brought on by a systemic breakdown of energy balance. It is a substantial risk factor for non-alcoholic fatty liver disease, diabetes, hypertension, and cardiovascular disease. Triglycerides gets accumulated in excessive amount in non-adipocytes and adipocytes which includes major organ like liver, pancreas and myocardium indicating important aspects of obesity. Increased abnormal levels of triglycerides causes risk by creating insulin resistance leading to diabetes mellitus, cardiomyopathy, and dyslipidaemia [2]. The relationship between the elevated levels of lipids and glucose control is interlinked through Acetyl-CoA metabolic pathway. In case of diabetes mellitus, the reduction in insulin secretion and lack of production of insulin by  $\beta$ -cells of pancreas are the important contributing factors. Early development of insulin is mainly caused due to the resistance to insulin, it is basically the lowered insulin signaling in tissue of liver, muscles and adipose [3]. Impaired glycogen synthesis and glucose uptake in skeletal muscle, abnormalities in glycogen synthesis, and elevated rates of gluconeogenesis in the liver are the major characteristics of insulin resistance [4-9]. Diacylglycerol O-acyl transferase-I (DGAT-I) catalyzes the final step of triglyceride synthesis as well as monitors the energy metabolism [10]. DGAT-I is responsible of conversion of diacylglycerol to triacylglycerol using fatty acid. DGAT -I inhibition in intestine is essential to improve various metabolic disorders. It has been observed in animal studies that DGAT-I inhibitors show desired effects in case of metabolic disorders. Many

DGAT-I inhibitors are reported and many are patented, which are still in clinical research. Drug like AZD7687 causes severe side effects like diarrhoea, leads to discontinuation of therapy in Phase I clinical trial and restricts its entry in Phase II [11]. One of the important reasons identified for the same is mutation occurring in DGAT-I, which prevents the development and research of DGAT-I inhibitors [12]. Pharmaceutical companies are developing novel chemical entity as selective DGAT-1 inhibitors with distinctive structural features, including, these companies are Hoffman-La Roche, AstraZeneca, Novartis, Pfizer, and Abbott. Looking into the structural characteristic of the reported DGAT-I inhibitors, novel molecules have been designed which will possess anti-diabetic activity and anti-obesity effect as well [13-17].

Drug development comprises establishing a target receptor hypothesis for a certain condition, screening the *in vitro* and/or *in vivo* biological activities of the new drug candidates, and evaluating the effectiveness and toxicity of the new drug candidates. Conducting DMPK (drug metabolism and pharmacokinetics) research, also known as ADMET (absorption, distribution, metabolism, elimination, and toxicity) investigations, is a crucial step in the discovery and development of new drugs. Early absorption, distribution, metabolism, and excretion (ADME) screening was used, and it has significantly reduced the percentage of substances failing clinical trials. Computer-aided drug discovery involves the *in vitro* ADME studies to predict the *in vivo* animal and human pharmacological effects outcomes. The result obtained through these studies is based on the database available in that computational tool, which is reliable and provides probability values of various parameters [18-19]. The preclinical study involves animal experimentation, which is time-consuming. Hence some of the newer *in vitro* studies are proposed to obtain the prediction of *in vivo* studies which can successfully reduce the use of experimental animals in research. Further *in vitro* studies reduce the time of research, control the variables, and offer flexibility to change them. ADMET predictions are useful and can minimize the number of molecules entering clinical trials. These predictions can also help to understand the drug likeliness, ligand likeliness, and synthetic accessibility during the wet lab.

## **2. MATERIAL AND METHODS:**

The 2D structures of all ligands were drawn in Chemdraw and 2D and 3D structures were energy-minimized using Maestro Schrodinger software. As per the requirement of the input file format for various software tools; the related smiles format, mol format, .sdf file formats were generated and applied for the investigation. For the determination of physicochemical properties, pharmacokinetic properties, lead likeliness, drug likeliness, and synthetic possibility of the newly designed ligands Swiss ADME was employed. All the results were retrieved in excel or csv file format and results were compared. Investigation of anti-diabetic activity and other related potential activities were predicted using PASS online database. Moinpiration was also utilized for the prediction of biological activity.

### **2.1 Physicochemical properties, pharmacokinetic properties, drug likeliness, ligand likeliness evaluation using SwissADME:**

A chemical compound or designed ligand must reach to its target in an appropriate concentration and remain there in its active state for it to manifest its activity. Only then will it be able to demonstrate its pharmacological effect. Therefore, it becomes crucial to assess the compounds ADME (Absorption, Distribution, Metabolism, and Excretion) before beginning the real experimental work. Computer software models can provide a great substitute for the assessment of the potential of the molecule as a therapeutically active molecule. Swiss ADME is free software tool available which uses smiles as input format and provides the number of characteristics of the molecule like physicochemical properties, pharmacokinetic characteristics, drug likeliness and ligand likeliness. Total 36 molecules were studied for investigating various properties including solubility, logP values etc (website <http://www.swissadme.ch/>). The proficient access provided by this SwissADME is iLogP values and BOILED-egg concept which decides the permeability of the compounds in biological environment. Swiss similarity, Swiss Target predication, SwissDock, Swiss bioisoster and Swiss Param are the computer aided drug design tools provided by SIB Swiss institute of bioinformatics. Structure of the molecule determines the drug likeliness of the molecule. Ghose, Veber, Egan, Muegge procedure and more widely employed Lipinski Rule of five is been employed during the analysis of the molecule. Table 1 contains the various ligands designed with isonicotinic acid, forming amino acid linkage, piperazine and phenyl

piperazine moiety with isomers of hydroxy benzoic acid. Table 2 contains derivatives designed with picolinic acid.

## **2.2 ADMET prediction using Molsoft pkCSM:**

pkCSM is another computational tool available for the determination of ADMET predictions. The web server available is [pkCSM \(uq.edu.au\)](http://pkCSM(uq.edu.au)). This method provides graph-based signatures. The co-relation between the pharmacokinetic properties, potency of molecule and toxicity is essential to study the effectiveness of the drug. Binding property of the ligand with receptor ensures that the molecule can reach to the target site [21].

## **2.3 Molecular Target Prediction:**


The Swiss Target Prediction service was used for studies on specific targets and offers an understanding about physiological side effects and cross reactivity for antidiabetic efficacy by inputting names of desired medications. To identify the likely targets of the presented molecule, a three-dimensional and two-dimensional similarity index with known ligands is applied.

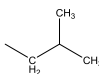
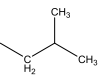
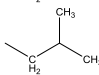
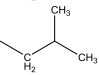
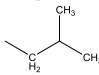
## **2.4 Biological activity spectra for ligands using Molinspiration:**


Cheminformatics software tools Molinspiration tool provide bioactivity prediction, data visualisation, 3D structure generation and fragment-based virtual screening.

## **2.5 Biological activity spectra for ligands using PASS online:**

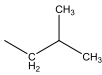
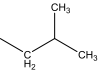
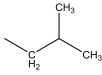
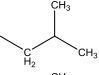
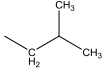
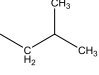
A free online tool called Prediction of Activity Spectra for Substances (PASS) [22]. forecasts the biological effects of compounds that resemble drugs (<http://www.way2drug.com/passonline>). It also forecasts a structure-activity relationship (SAR) based on multilevel neighbourhoods of atom (MNA) descriptors and a modified Bayesian algorithm encompassing more than 300,000 organic compounds with more than 6,825 different biological activities. As a result, PASS may be used to enhance and focus biological testing and chemical synthesis. The results are reported indicates the anti-diabetic activity, insulin sensitizer, insulin secretagogue, diacylglycerol-o-acyl transferase inhibitor activity of the newly designed ligands INA1, INA11, INA13, INAPP21, PA2, PA9, PAPP25, PAPP30. Probable activity is denoted by Pa and probable inactivity is denoted Pi.

**Table1: Structures of Nicotinic acid derivatives designed based on above Hypothesis**


Sr. No	Compound Code	R <sub>1</sub>	R <sub>2</sub>	Sr. No	Compound Code	R <sub>1</sub>	R <sub>2</sub>
1	INA 01	-CH <sub>3</sub>	2-hydroxy Benzoic acid	11	INAPP18	-CH <sub>3</sub>	3-hydroxy Benzoic acid
2	INA 02	-CH <sub>3</sub>	3-hydroxy Benzoic acid	12	INAPP21	-H	2-hydroxy Benzoic acid
3	INA 03	-CH <sub>3</sub>	4-hydroxy Benzoic acid	13	INAPP22	-H	3-hydroxy Benzoic acid
4	INA 05	-H	2-hydroxy Benzoic acid	14	INAPP23	-H	4-hydroxy Benzoic acid
5	INA 07	-H	3-hydroxy Benzoic acid	15	INAPP25		2-hydroxy Benzoic acid
6	INA 11		4-hydroxy Benzoic acid	16	INAPP27		4-hydroxy Benzoic acid
7	INA 12		4-amino Benzoic acid	17	INAPP28		4-amino Benzoic acid
8	INA 13	-CH <sub>2</sub> OH	2-hydroxy Benzoic acid				
9	INA 15	-CH <sub>2</sub> OH	4-hydroxy Benzoic acid				
10	INA 16	-CH <sub>2</sub> OH	4-amino Benzoic acid				

**Table 2: Structures of Picolinic acid derivatives designed based on above Hypothesis**


Sr. No	Compound Code	R <sub>1</sub>	R <sub>2</sub>	Sr. No	Compound Code	R <sub>1</sub>	R <sub>2</sub>
18	PA1	-CH <sub>3</sub>	2-hydroxy Benzoic acid	28	PAPP17	-CH <sub>3</sub>	2-hydroxy Benzoic acid
19	PA2	-CH <sub>3</sub>	3-hydroxy Benzoic acid	29	PAPP18	-CH <sub>3</sub>	3-hydroxy Benzoic acid
20	PA3	-CH <sub>3</sub>	4-hydroxy Benzoic acid	30	PAPP19	-CH <sub>3</sub>	4-hydroxy Benzoic acid
21	PA5	-H	2-hydroxy Benzoic acid	31	PAPP21	-H	2-hydroxy Benzoic acid
22	PA6	-H	3-hydroxy Benzoic acid	32	PAPP24	-H	4-amino Benzoic acid

23	PA7	-H	4-hydroxy Benzoic acid	33	PAPP25		2-hydroxy Benzoic acid
24	PA9		2-amino Benzoic acid	34	PAPP26		3-hydroxy Benzoic acid
25	PA11		4-hydroxy Benzoic acid	35	PAPP27		4-hydroxy Benzoic acid
26	PA12		4-amino Benzoic acid	36	PAPP30	-CH <sub>2</sub> OH	3-hydroxy Benzoic acid
27	PA15	-CH <sub>2</sub> OH	4-amino Benzoic acid				

### 3. Result and Discussion:

#### 3.1 Physicochemical, pharmacokinetic and drug likeliness properties:

36 molecules and the reported DGAT-I inhibitor AZD3988 2D structures were drawn in Chemdraw software and copied in the form of smile. By putting these smiles in Swiss ADME [19], the various pharmacokinetic properties of the novel ligands are obtained. In Table 3, the SMILE format and molecular weight of the ligands is presented. ADME predictions were run for all 37 molecules and from these 37 molecules the bioavailability radar was obtained for each molecule. Depending on the ADME values obtained and comparing the RADAR charts, the molecules were grouped together and the best representing molecule with maximum ideal properties which follow Lipinski rule of 5, better GI absorption, BBB permeability, solubility parameters etc. were selected and the related data is presented in Table 4. The molecules INA1(Molecule 1), INA11 (Molecule 6), INA13 (Molecule 8), INAPP21(Molecule 12), PA2 (Molecule 19), PA9, (Molecule 24), PAPP25 (Molecule 33), PAPP30 (Molecule 36) were selected and the results are presented. It has observed that the representing molecule from each group present, INA1(Molecule 1), INA11 (Molecule 6), INA13 (Molecule 8), INAPP21(Molecule 12), PA2 (Molecule 19), PA9, (Molecule 24), PAPP25 (Molecule 33), PAPP30 (Molecule 36) have ideal number of hydrogen bond donor value less than 5 and hydrogen bond acceptors value less than 5. A topological polar surface area (TPSA), fragmental strategy which consider P (phosphorus) and S (sulphur) polar atoms estimated the PSA values. Total polar surface area of 6 molecules out of 8 is nearby the reported DGAT-I inhibitor AZD3988. All the molecules show high gastro-intestinal absorption. None of the molecule is permeable to blood brain barrier. Bioavailability of score for all the molecules is same as that of AZD 3988. These values provides the applicability of the designed ligands to be drug molecules showing better lead likeliness values and Swiss ADME Synthetic Accessibility (SA) Score. For common chemical moieties and unfavourable for rare moieties, the fragmental impact on SA ought to be favourable. Synthetic accessibility score was also close to the existing DGAT-I inhibitor, which will help to take these molecules for synthesis. Only two molecules 33, 36 show PAINS alert, indicating violation from specific nature of the molecule.

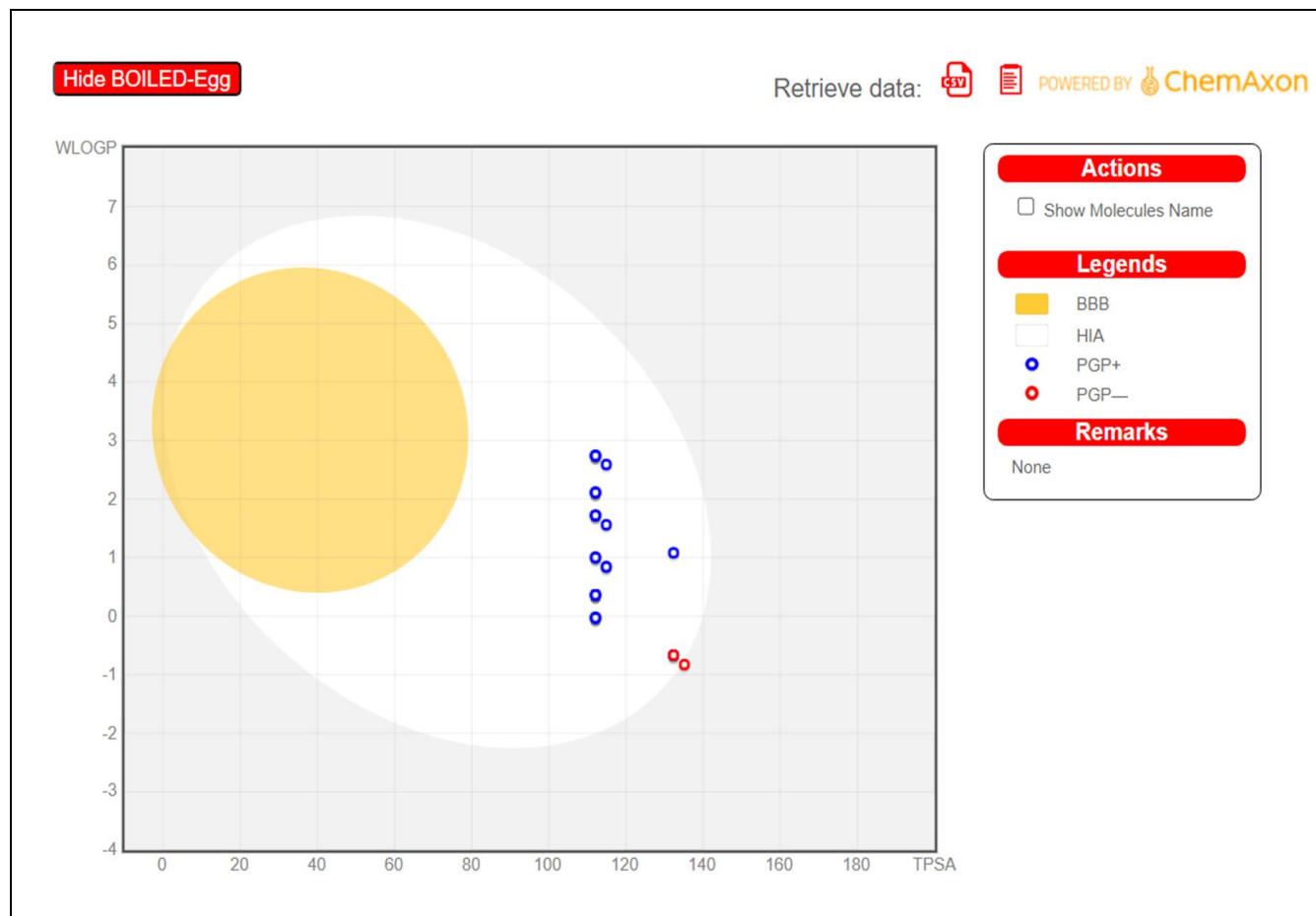
**Table 3: The canonical smiles for all 36 structures and reported DGAT-I inhibitor AZD3988**

Molecule	Canonical smile format	Molecular formula
1	<chem>CC(C(=O)N1CCN(CC1)CCOc1cccc1C(=O)O)NC(=O)c1ccncc1</chem>	C22H26N4O5
2	<chem>CC(C(=O)N1CCN(CC1)CCOc1ccc(c1)C(=O)O)NC(=O)c1ccncc1</chem>	C22H26N4O5
3	<chem>CC(C(=O)N1CCN(CC1)CCOc1ccc(cc1)C(=O)O)NC(=O)c1ccncc1</chem>	C22H26N4O5
4	<chem>O=C(N1CCN(CC1)CCOc1cccc1C(=O)O)CNC(=O)c1ccncc1</chem>	C21H24N4O5
5	<chem>O=C(N1CCN(CC1)CCOc1ccc(cc1)C(=O)O)CNC(=O)c1ccncc1</chem>	C21H24N4O5
6	<chem>CC(C(C(=O)N1CCN(CC1)CCOc1ccc(cc1)C(=O)O)NC(=O)c1ccncc1)C</chem>	C24H30N4O5
7	<chem>CC(C(C(=O)N1CCN(CC1)CCNc1ccc(cc1)C(=O)O)NC(=O)c1ccncc1)C</chem>	C24H31N5O4
8	<chem>OCC(C(=O)N1CCN(CC1)CCOc1cccc1C(=O)O)NC(=O)c1ccncc1</chem>	C22H26N4O6
9	<chem>OCC(C(=O)N1CCN(CC1)CCOc1ccc(cc1)C(=O)O)NC(=O)c1ccncc1</chem>	C22H26N4O6
10	<chem>OCC(C(=O)N1CCN(CC1)CCNc1ccc(cc1)C(=O)O)NC(=O)c1ccncc1</chem>	C22H27N5O5
11	<chem>O=C(C(NC(=O)c1ccncc1)C)N1CCN(CC1)c1ccc(cc1)CCOc1cccc(c1)C(=O)O</chem>	C28H30N4O5
12	<chem>O=C(N1CCN(CC1)c1ccc(cc1)CCOc1cccc1C(=O)O)CNC(=O)c1ccncc1</chem>	C27H28N4O5
13	<chem>O=C(N1CCN(CC1)c1ccc(cc1)CCOc1ccc(c1)C(=O)O)CNC(=O)c1ccncc1</chem>	C27H28N4O5
14	<chem>O=C(N1CCN(CC1)c1ccc(cc1)CCOc1ccc(cc1)C(=O)O)CNC(=O)c1ccncc1</chem>	C27H28N4O5
15	<chem>CC(C(C(=O)N1CCN(CC1)c1ccc(cc1)CCOc1cccc1C(=O)O)NC(=O)c1ccncc1)C</chem>	C30H34N4O5
16	<chem>CC(C(C(=O)N1CCN(CC1)c1ccc(cc1)CCOc1ccc(cc1)C(=O)O)NC(=O)c1ccncc1)C</chem>	C30H34N4O5
17	<chem>CC(C(C(=O)N1CCN(CC1)c1ccc(cc1)CCNc1ccc(cc1)C(=O)O)NC(=O)c1ccncc1)C</chem>	C30H35N5O4
18	<chem>O=C(C(NC(=O)c1cccn1)C)N1CCN(CC1)CCOc1cccc1C(=O)O</chem>	C22H26N4O5
19	<chem>CC(C(=O)N1CCN(CC1)CCOc1cccc(c1)C(=O)O)NC(=O)c1cccn1</chem>	C22H26N4O5
20	<chem>O=C(C(NC(=O)c1cccn1)C)N1CCN(CC1)CCOc1ccc(cc1)C(=O)O</chem>	C22H26N4O5
21	<chem>O=C(N1CCN(CC1)CCOc1cccc1C(=O)O)CNC(=O)c1cccn1</chem>	C21H24N4O5
22	<chem>O=C(N1CCN(CC1)CCOc1ccc(c1)C(=O)O)CNC(=O)c1cccn1</chem>	C21H24N4O5
23	<chem>O=C(N1CCN(CC1)CCOc1ccc(cc1)C(=O)O)CNC(=O)c1cccn1</chem>	C21H24N4O5
24	<chem>CC(C(C(=O)N1CCN(CC1)CCOc1cccc1C(=O)O)NC(=O)c1cccn1)C</chem>	C24H30N4O5
25	<chem>CC(C(C(=O)N1CCN(CC1)CCOc1ccc(cc1)C(=O)O)NC(=O)c1cccn1)C</chem>	C24H30N4O5
26	<chem>CC(C(C(=O)N1CCN(CC1)CCNc1ccc(cc1)C(=O)O)NC(=O)c1cccn1)C</chem>	C24H31N5O4
27	<chem>OCC(C(=O)N1CCN(CC1)CCOc1ccc(cc1)C(=O)O)NC(=O)c1cccn1</chem>	C22H26N4O6
28	<chem>O=C(C(NC(=O)c1cccn1)C)N1CCN(CC1)c1ccc(cc1)CCOc1cccc1C(=O)O</chem>	C28H30N4O5
29	<chem>O=C(C(NC(=O)c1cccn1)C)N1CCN(CC1)c1ccc(cc1)CCOc1ccc(c1)C(=O)O</chem>	C28H30N4O5
30	<chem>O=C(C(NC(=O)c1cccn1)C)N1CCN(CC1)c1ccc(cc1)CCOc1ccc(cc1)C(=O)O</chem>	C28H30N4O5
31	<chem>O=C(N1CCN(CC1)c1ccc(cc1)CCOc1cccc1C(=O)O)CNC(=O)c1cccn1</chem>	C27H28N4O5
32	<chem>O=C(N1CCN(CC1)c1ccc(cc1)CCNc1ccc(cc1)C(=O)O)CNC(=O)c1cccn1</chem>	C27H29N5O4
33	<chem>CC(C(C(=O)N1CCN(CC1)c1ccc(cc1)CCOc1cccc1C(=O)O)NC(=O)c1cccn1)C</chem>	C30H34N4O5
34	<chem>CC(C(C(=O)N1CCN(CC1)c1ccc(cc1)CCOc1ccc(c1)C(=O)O)NC(=O)c1cccn1)C</chem>	C30H34N4O5
35	<chem>CC(C(C(=O)N1CCN(CC1)c1ccc(cc1)CCOc1ccc(cc1)C(=O)O)NC(=O)c1cccn1)C</chem>	C30H34N4O5
36	<chem>OCC(C(=O)N1CCN(CC1)c1ccc(cc1)CCOc1ccc(c1)C(=O)O)NC(=O)c1cccn1</chem>	C28H30N4O6
37	<chem>OC(=O)CC1CCC(CC1)c1ccc(cc1)NC(=O)c1nnc(o1)Nc1ccc(c(c1)F)F</chem>	C23H22F2N4O4



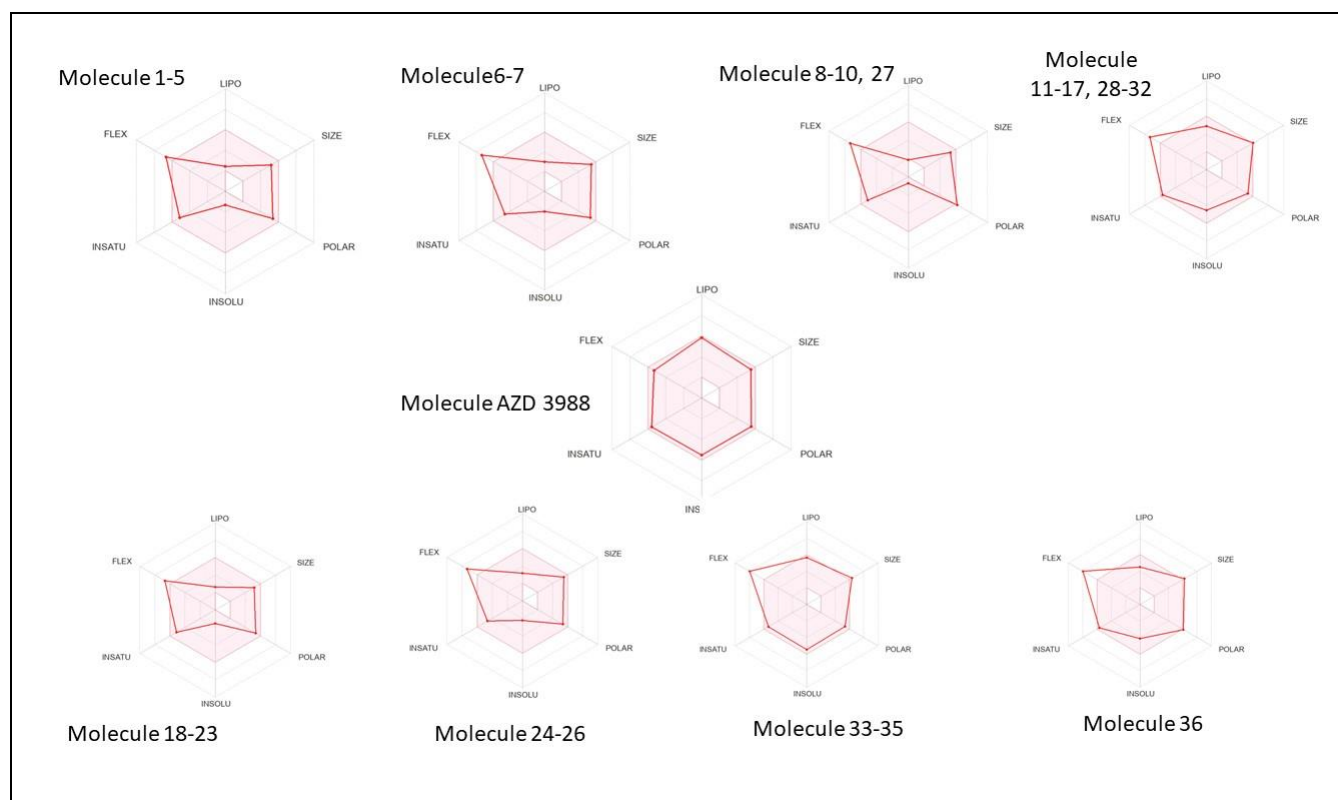
**Table 4: The physicochemical, pharmacokinetic and drug likeliness predictions of 8 representing molecule and reported DGAT-I inhibitor AZD3988**

	H-bond acceptor	H-bond donors	TPSA	CYP1A2 inhibitor	CYP2C19 inhibitor	CYP2C9 inhibitor	CYP2D6 inhibitor	CYP3A4 inhibitor	GI absorption	BBB permeant	Lipinski violations	Bioavailability Score	PAINS alerts	Leadlikeness violations	Synthetic Accessibility
Molecule 1	7	2	11 2.07	No	No	No	No	No	High	No	0	0.55	0	2	3.27
Molecule 6	7	2	11 2.07	No	No	No	No	No	High	No	0	0.55	0	2	3.37
Molecule 8	8	3	13 2.3	No	No	No	No	No	High	No	0	0.55	0	2	3.39
Molecule 12	6	2	11 2.07	No	Yes	Yes	Yes	Yes	High	No	0	0.56	1	2	3.2
Molecule 19	7	2	11 2.07	No	No	No	No	No	High	No	0	0.55	0	2	3.34
Molecule 24	7	2	11 2.07	No	No	No	No	No	High	No	0	0.55	0	2	3.54
Molecule 33	6	2	11 2.07	No	Yes	Yes	Yes	Yes	High	No	1	0.56	1	3	4
Molecule 36	7	3	13 2.3	No	Yes	Yes	Yes	Yes	High	No	1	0.56	1	2	3.91
AZD3988	8	3	11 7.35	No	No	Yes	No	No	Low	No	0	0.56	0	3	4.09



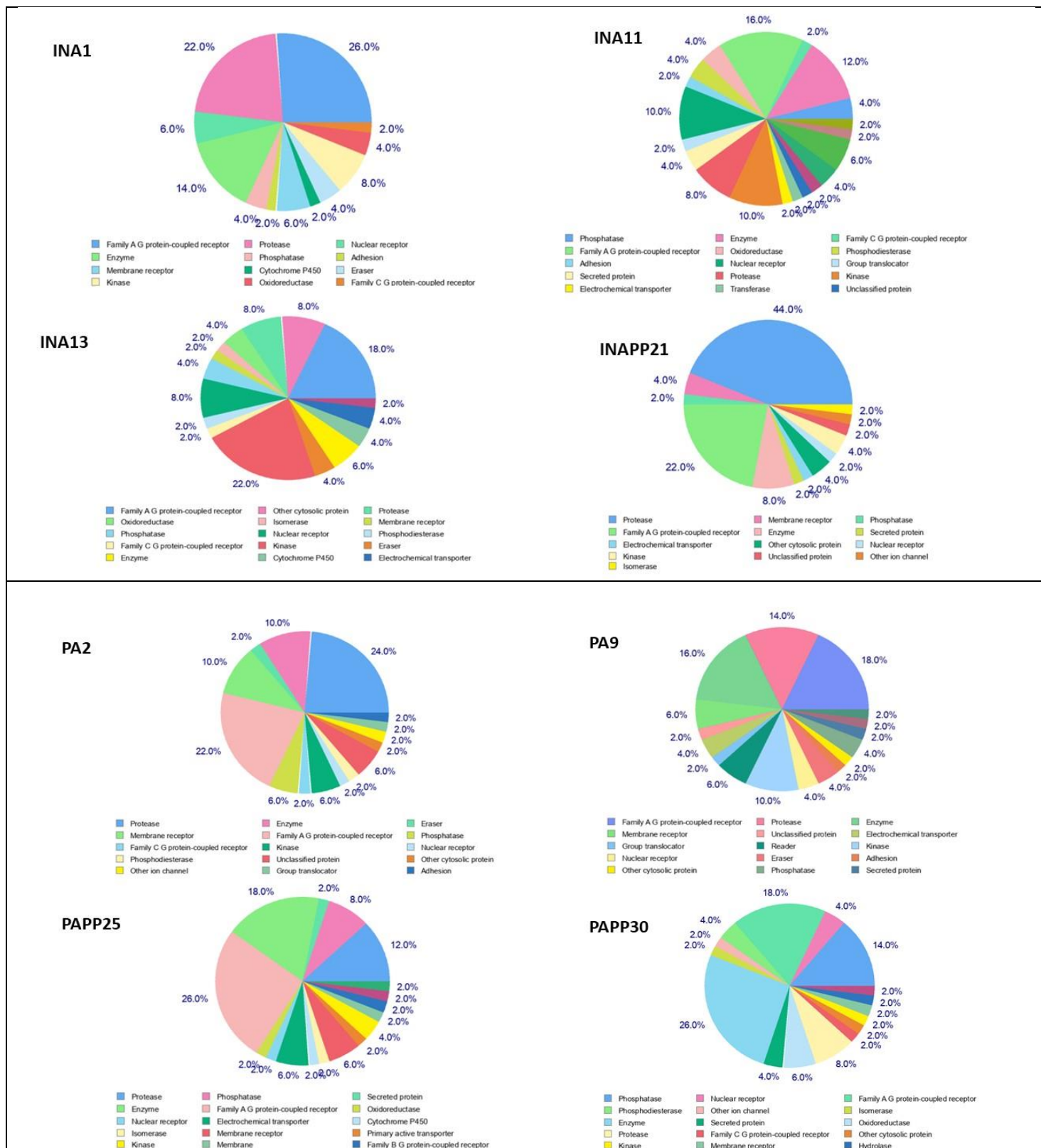
**Figure 2: Egg's yolk predictions for permeability of molecules into blood-brain barrier**

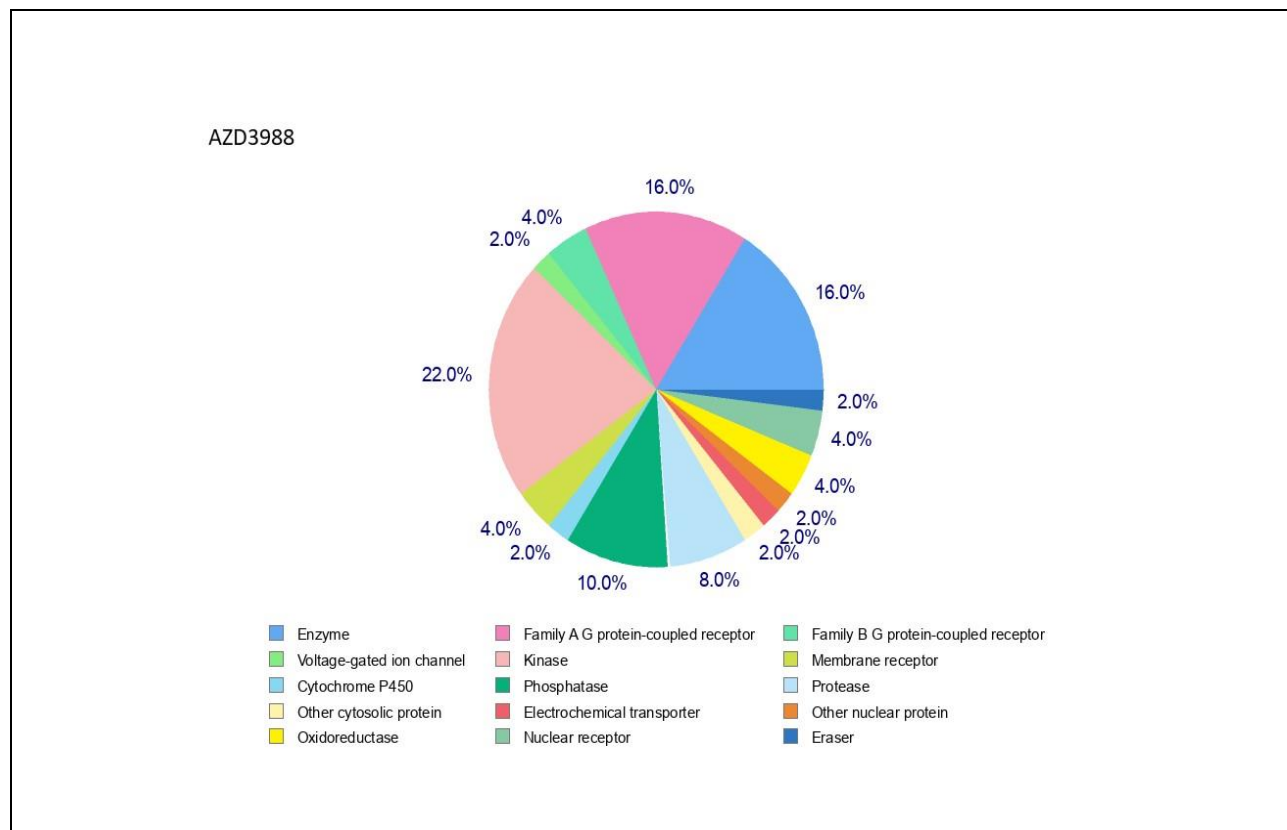
The boiled egg model (Figure 2), which was used to study the pharmacokinetic features, enables intuitive assessment of passive GI absorption (HIA) and brain penetration (BBB), depending on the location of the molecules in the WLOGP-versus-TPSA reference space [20]. The yellow portion (yolk) is for a substantial chance of brain penetration, while the white part is for high possibility of passive absorption through the gastrointestinal system. Yolk and white regions are not incompatible. P-glycoprotein plays very important role in absorption of the drug where only two molecules are devoid of p-glycoprotein conjugation. P-glycoprotein does not appear to increase the excretion of drugs out of hepatocytes and renal tubules into the surrounding luminal space, but rather appears to restrict the cellular absorption of drugs from blood circulation into the brain and from intestinal lumen into epithelial cells. Out of all 36 designed ligands, all drugs do not cross the blood brain barrier.



**Figure 3: Bioavailability radar presenting reported DGAT-I inhibitor and summarized designed ligand using Swiss ADME Predictor**

Figure 3 showed bioavailability radar where suitable physicochemical space is indicated with colored zone emphasize on oral bioavailability considering the lipophilicity, size, polarity, solubility, insolubility, saturation, flexibility. The ideal molecular weight for the molecule must range from 150 g/mol to 500g/mol. The bioavailability radar is representing the group of molecule which are showing same type of radar. Radar 1 contains the molecules from 1 to 6, radar 2 contains 77molecule 6 & 7, radar 3 indicates molecule 8-10 & 27, radar 4 indicates molecule 11-17 & 28-32, radar 5 indicates molecule 18-23, radar 6 indicates molecule 24-26, radar 7 indicates molecule 33-35 and radar 8 indicates the last unique molecule 36. At the centre of the figure the radar figure of AZD 3988 is shown for the comparative purpose. So it is observed that the molecules 11-17, 28-32,33-35 and 36 are showing nearer radar that is relative bioavailability to that of standard/reported DGAT-I inhibitor AZD 3988.



**Figure 4. Pie-chart of top-50 of target predicted for designed ligand INA1, INA11, INA13, INAPP21, PA2, PA9, PAPP25, PAPP30****Figure 5. Pie-chart of top-50 of target predicted for AZD3988**

### 3.2 Target prediction:

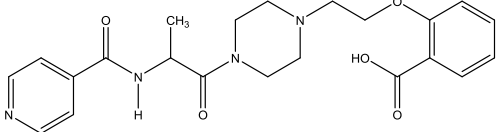
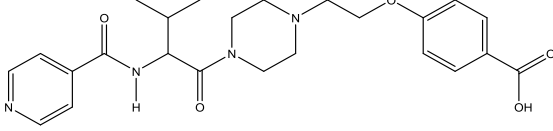
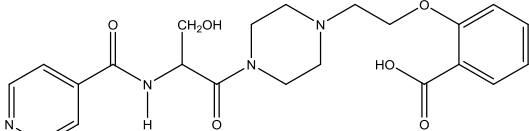
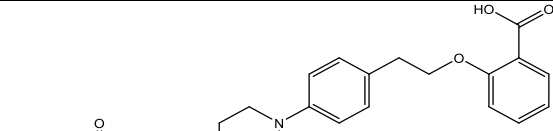
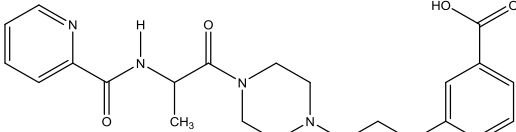
Based on their similarity to existing chemicals, molecular target studies were predicted to estimate their targets, analyse the molecular mechanisms behind a certain phenotypic or bioactivity, and rationalise any adverse effects. Based on Target, Common Name, Uniprot ID, ChEMBL-ID, and Top 50 Results of the Closely Related Receptors in 2D/3D are shown in pie chart. Here in Figure 4 all pie charts of 8 molecules IAN1, INA11, INA13, INAPP21, PA2, PA9, PAPP25, PAPP30 is shown and in figure 5 pie chart for AZD 3988 interactions with top 50 receptors is shown. The reported AZD 3988 DGAT-I inhibitors show 22% kinase inhibitory activity, 16% Family A G protein coupled receptor activity, 16% enzyme inhibitory activity. INA1 also shows 26% kinase inhibitory activity, 22% protease inhibitory activity and 14% enzyme inhibitory activity. INA11 shows 16% Family A G protein coupled receptor, 12% enzyme inhibitory activity. INA13 shows

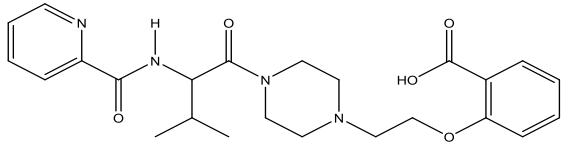
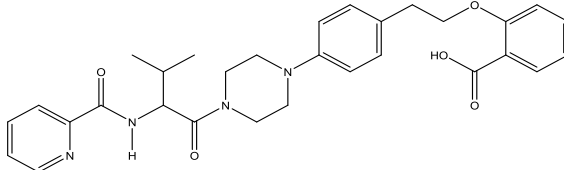
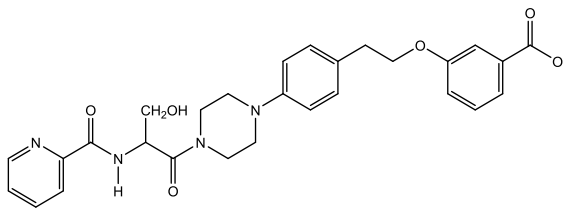
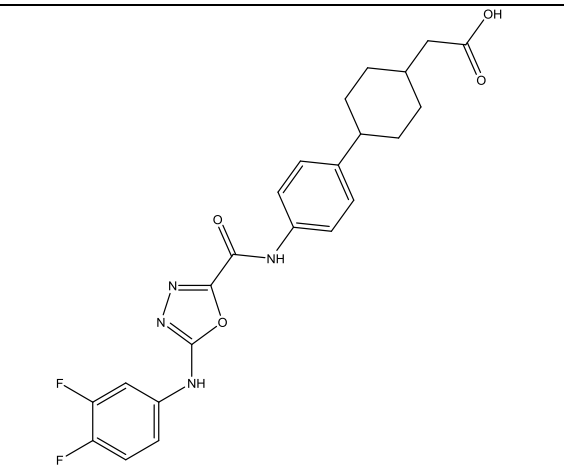
22% kinase inhibitory activity and 18% Family A G protein coupled receptor binding. INAPP21 shows 44% of protease inhibitory activity and 22% Family A G protein coupled receptor binding. PA2 shows 24% protease inhibitory activity and 22% Family A G protein coupled receptor binding. Molecule PA9 shows 18 % of Family A G protein coupled receptor binding, 16% of enzyme inhibitory activity, 14 % of protease inhibitory activity. PAPP25 shows 26% of Family A G protein coupled receptor activity, 18% of enzyme inhibitory activity, 12% of protease inhibitory activity. PAPP30 shows 26% enzyme inhibitory activity, 18% and 14% of phosphatase activity. In the case of AZD3988 it shows 22% of kinase inhibitory activity, 16% of Family A G protein-coupled receptor binding, 16% of enzyme inhibitory activity. The designed molecules are showing quite comparable results to that of AZD3988 molecule.

### **3.3 PASS predictions:**

PASS online predictions provide insights into the probable active or probable inactivity of the molecule for certain diseases giving the biological spectrum. The maximum similarity score 1 the values are calculated. The values obtained for the 08 representing molecule are presented in Table 5. Molecule INA1 indicates the active coefficient of 0.580, 0.260, 0.154 as an insulin promotor, anti-diabetic and insulin sensitizer. INA11 shows 0.650, 0.354, 0.147 as insulin promotors, lipid metabolism regulators and type 2 anti-diabetic agents. INA13 shows the coefficient of 0.563, 0.351, 0.219 as insulin promotor, lipid metabolism regulators and anti-diabetic. INAPP21 shows 0.633, 0.480 , 0.435 as insulin promotor and anti-diabetic activity. PA2 shows the activity coefficients 0.505, 0.265,0.179 as insulin promotor and anti-diabetic activity. PA9 indicates the 0.722, 0.161 as insulin promotor and anti-diabetic activity. PAPP25 shows interesting values for coefficient as 0.834, 0.297,0.281 as insulin promotor, apoptosis antagonist and anti-diabetic activity. While the PAPP30 shows the values of 0.645, 0.327,0.217 as insulin promotor and anti-diabetic activity. AZD 3988 also shows active coefficient as 0.858, 0.735, 0.579 for diacylglycerol o-acyl transferase, anti-obesity and anti-diabetic activity.

Table 5: PASS prediction of Anti-diabetic activity of selected ligands and AZD3988

Sr. No.	Name of Compound	Chemical Structures	Pa	Pi	Activity and percentage Activity
1.	INA 01	 2-(2-(4-(isonicotinoylalanyl)piperazin-1-yl)ethoxy)benzoic acid	0,580 0,525 0,271 0,260 0,176 0,207 0,154 0,185 0,133	0,017 0,081 0,059 0,107 0,027 0,069 0,024 0,066 0,039	Insulin promoter Kidney function stimulant Antidiabetic symptomatic Antidiabetic Diabetic retinopathy treatment Pancreatic disorders treatment Insulin sensitizer Antidiabetic (type 2) Insulin secretagogues
2.	INA 11	 4-(2-(4-(isonicotinoylvalyl)piperazin-1-yl)ethoxy)benzoic acid	0,650 0,538 0,354 0,156 0,147 0,187	0,009 0,073 0,114 0,048 0,089 0,147	Insulin promoter Kidney function stimulant Lipid metabolism regulator Diabetic retinopathy treatment Antidiabetic (type 2) Antidiabetic symptomatic
3.	INA 13	 2-(2-(4-(isonicotinoylseryl)piperazin-1-yl)ethoxy)benzoic acid	0,564 0,492 0,351 0,179 0,284 0,219	0,019 0,102 0,115 0,024 0,152 0,104	Insulin promoter Kidney function stimulant Lipid metabolism regulator Diabetic retinopathy treatment Insulysin inhibitor Antidiabetic symptomatic
4.	INAPP21	 2-(4-(4-(isonicotinoyl)glycyl)piperazin-1-yl)phenethoxy)benzoic acid	0,633 0,480 0,435 0,171 0,214 0,138 0,209 0,123 0,228 0,165	0,011 0,026 0,015 0,031 0,109 0,033 0,106 0,036 0,188 0,160	Insulin promoter Antidiabetic Antidiabetic (type 2) Diabetic retinopathy treatment Antidiabetic symptomatic Insulin secretagogues Apoptosis antagonist Insulin sensitizer Lipid metabolism regulator Antiobesity
5.	PA2	 3-(2-(4-(picolinoylalanyl)piperazin-1-yl)ethoxy)benzoic acid	0,505 0,332 0,265 0,227 0,179 0,147 0,113	0,028 0,096 0,063 0,027 0,027 0,089 0,065	Insulin promoter Lipoprotein lipase inhibitor Antidiabetic symptomatic Antihyperlipoproteinemic Antidiabetic (type 1) Antidiabetic (type 2) Insulin secretagogues

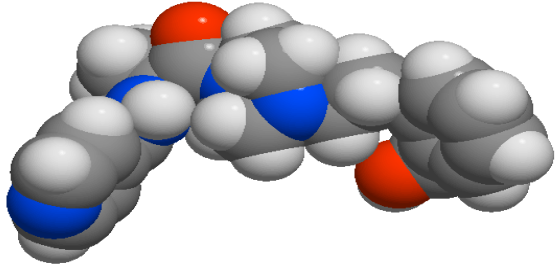
6.	PA 9	 <p>2-(2-(4-(picolinoylvalyl)piperazin-1-yl)ethoxy)benzoic acid</p>	0,722 0,251 0,272 0,161 0,156 0,216 0,307 0,135 0,137 0,217	0,005 0,036 0,132 0,042 0,046 0,107 0,199 0,031 0,034 0,144	Insulin promoter Pancreatic disorders treatment Lipoprotein lipase inhibitor Diabetic retinopathy treatment Antidiabetic (type 1) Antidiabetic symptomatic Diabetic neuropathy treatment Insulin sensitizer Insulin secretagogues Antidiabetic
7.	PAPP25	 <p>2-(4-(4-(picolinoylvalyl)piperazin-1-yl)phenethoxy)benzoic acid</p>	0,834 0,297 0,281 0,289 0,232 0,148 0,145 0,146 0,144	0,004 0,032 0,035 0,088 0,048 0,026 0,027 0,060 0,066	Insulin promoter Apoptosis antagonist Antidiabetic (type 2) Antidiabetic Pancreatic disorders treatment Insulin sensitizer Insulin secretagogues Antidiabetic (type 1) Diabetic retinopathy treatment
8.	PAPP30	 <p>3-(4-(4-(picolinoylseryl)piperazin-1-yl)phenethoxy)benzoic acid</p>	0,645 0,394 0,327 0,225 0,217 0,183 0,155 0,101 0,080	0,010 0,090 0,069 0,053 0,052 0,024 0,049 0,047 0,053	Insulin promoter Insulysin inhibitor Antidiabetic Pancreatic disorders treatment Antidiabetic (type 2) Antidiabetic (type 1) Diabetic retinopathy treatment Insulin sensitizer Diacylglycerol O-acyltransferase inhibitor
9.	AZD3988	 <p>2-(4-(5-((3,4-difluorophenyl)amino)-1,3,4-oxadiazole-2-carboxamido)phenyl)cyclohexyl)acetic acid</p>	0,858 0,735 0,609 0,579 0,211	0,001 0,005 0,001 0,014 0,054	Diacylglycerol O-acyltransferase inhibitor Antiobesity Diacylglycerol O-acyltransferase 1 inhibitor Antidiabetic Antidiabetic (type 2)



**3.4 Biological Activity Predictions using Molinspiration software:**

The mol files of the 08 representing molecules were submitted to Molinspiration 3D structures of molecules were generated and 3D structure of INA1 is shown in Table 6. While the comparative values obtained for the biological activities of these molecules is provided in Table 7. The comparative study indicates that PAPP30 is having maximum interaction with G-protein coupled receptor (GPCR) with value 0.32. INA13 with value of 0.06 is having more affinity for ion channel modulators. INA13 and PAPP30 show similar kinase inhibitory activity as 0.11, which is nearer to AZD3988 having value 0.15. PAPP30 is having nuclear receptor ligand interaction value more as compared to other molecules as 0.04. Molecules INA1, INA11, INA13, PA2, PA9, PAPP25, PAPP30 shows higher protease inhibitory activity (0.25, 0.28, 0.32, 0.28, 0.34, 0.33, 0.33 respectively) as compared to AZD 3988 with 0.23. While INA13 with value 0.15 and PAPP30 with value 0.18 for enzyme inhibitor is greater than that of AZD 3988 with value 0.11. Figure 6 indicates the graphical presentation of comparative study of biological activity predictions given by Molinspiration.

**Table 6: 3D image of INA1 obtained from Molinspiration and biological activity**

	<u>Molinspiration</u>	<u>bioactivity</u>	<u>score</u>
	v2022.08		
	GPCR ligand	0.21	
	Ion channel modulator	-0.02	
	Kinase inhibitor	0.05	
	Nuclear receptor ligand	-0.12	
	Protease inhibitor	0.25	
	Enzyme inhibitor	0.05	

**Table 7: Comparative Table of Biological activity obtained for selected ligands and AZD3988**

Name of parameter	INA1	INA11	INA 13	INAPP21	PA2	PA9	PAPP25	PAPP30	AZD3988
GPCR ligand	0.21	0.15	0.28	0.19	0.24	0.24	0.26	0.32	0.05
Ion channel modulator	-0.02	-0.07	0.06	-0.04	-0.01	-0.03	-0.14	0	-0.13
Kinase inhibitor	0.05	0.03	0.11	0.05	0.06	0.07	0.05	0.11	0.15
Nuclear receptor ligand	-0.12	-0.1	-0.02	-0.05	-0.08	-0.11	-0.09	0.04	-0.05
Protease inhibitor	0.25	0.28	0.32	0.17	0.28	0.34	0.33	0.33	0.23
Enzyme inhibitor	0.05	0.05	0.15	0.05	0.08	0.1	0.08	0.18	0.11

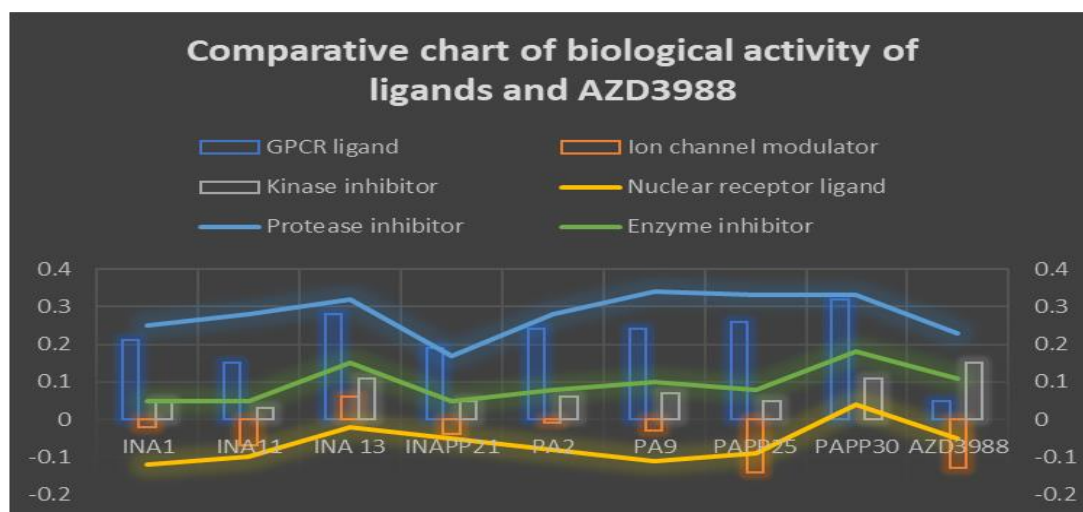


**Figure 6: Comparative chart of biological activity obtained from Molinspiration software tool**

### 3.5 ADMET predictions by pkCSM:

The SMILES format of the molecules were submitted to the pkCSM tool and predictions obtained for best 08 molecules are presented in Table 8. Skin permeability of all designed ligands are as equal to AZD 3988. The unique characteristic observed with this study is values for Oral Rat Acute Toxicity (LD50) value, Oral Rat Chronic Toxicity values which are quite similar to that of standard/reference drug AZD 3988.

**Table 8: ADMET predictions obtained from pkCSM Molsoft Tool**

Sr. No.	Property	Model Name	Predicted Value								
			INA 01	INA 11	INA 13	INAPP18	PA2	PA9	PAPP25	PAPP30	AZD3988
1	Absorption	Water solubility (log mol/L)	-3.195	-3.209	-3.165	-3.761	-2.963	-3.26	-3.631	-3.431	-4.122
2	Absorption	Caco2 permeability (log P in 10-6 cm/s)	0.57	0.22	0.466	0.781	0.475	0.664	0.679	0.515	-0.068
3	Absorption	Intestinal absorption (human) %	49.494	52.943	39.867	56.394	54.317	50.524	59.637	53.787	83.368
4	Absorption	Skin Permeability (log Kp)	-2.735	-2.735	-2.735	-2.734	-2.735	-2.735	-2.735	-2.735	-2.735
5	Absorption	P-glycoprotein substrate	Yes	Yes	Yes	Yes	Yes	Yes	Yes	Yes	Yes
6	Absorption	P-glycoprotein I inhibitor	No	No	No	No	No	No	No	No	No
7	Absorption	P-glycoprotein II inhibitor	No	No	No	No	No	No	No	No	Yes
8	Distribution	VDss (human) (log L/kg)	-1.075	-1.104	-1.184	-1.813	-1.164	-1.082	-1.763	-1.873	-0.994
9	Distribution	Fraction unbound (human) (Fu)	0.406	0.288	0.434	0	0.434	0.353	0	0.021	0.003
10	Distribution	BBB permeability (log BB)	-1.014	-1.003	-1.119	-1.183	-1.033	-1.022	-1.025	-1.134	-1.584
11	Distribution	CNS permeability (log PS)	-3.843	-3.724	-4.168	-3.43	-3.857	-3.711	-3.397	-3.863	-3.043
12	Metabolism	CYP2D6 substrate	No	No	No	No	No	No	No	No	No
13	Metabolism	CYP3A4 substrate	No	No	No	No	No	No	No	No	Yes
14	Metabolism	CYP1A2 inhibitor	No	No	No	No	No	No	No	No	Yes

15	Metabolism	CYP2C19 inhibitor	No	No	No	No	No	No	No	No	No
16	Metabolism	CYP2C9 inhibitor	No	No	No	No	No	No	No	No	Yes
17	Metabolism	CYP2D6 inhibitor	No	No	No	No	No	No	No	No	No
18	Metabolism	CYP3A4 inhibitor	No	No	No	No	No	No	No	No	No
19	Excretion	Total Clearance (log ml/min/kg)	0.267	0.229	0.296	0.646	0.302	0.058	0.55	0.442	-0.267
20	Excretion	Renal OCT2 substrate	No	No	No	No	No	No	No	No	No
21	Toxicity	AMES toxicity	No	No	No	No	No	No	No	No	No
22	Toxicity	Max. tolerated dose (human) (log mg/kg/day)	1.204	0.853	1.217	1.188	0.805	1.222	1.26	0.859	-0.055
23	Toxicity	hERG I inhibitor	No	No	No	No	No	No	No	No	No
24	Toxicity	hERG II inhibitor	No	No	No	No	No	No	No	No	No
25	Toxicity	Oral Rat Acute Toxicity (LD50) (mol/kg)	2.057	2.192	1.913	2.832	2.134	2.13	3.092	2.951	2.684
26	Toxicity	Oral Rat Chronic Toxicity (LOAEL) (log mg/kg_bw/day)	1.719	1.934	1.773	1.594	1.678	1.786	2.043	2.004	2.046
27	Toxicity	Hepatotoxicity	Yes	Yes	Yes	Yes	Yes	Yes	Yes	Yes	Yes
28	Toxicity	Skin Sensitisation	No	No	No	No	No	No	No	No	No
29	Toxicity	<i>T.Pyiformis</i> toxicity (log ug/L)	0.285	0.285	0.285	0.286	0.285	0.285	0.285	0.285	0.286
30	Toxicity	Minnow toxicity (log mM)	3.384	2.874	3.863	1.955	3.464	3.065	1.446	2.45	-0.064

#### 4. Conclusion:

Total 36 newly designed molecules were submitted to computational investigation of ADMET studies using Swiss ADME, pkCSM ADMET predictions, Swiss target prediction, biological activity using Molinspiration. The values obtained are quite promising and the gives idea about the physicochemical, pharmacokinetic, pharmacological aspects of newly designed ligands. These molecules are found to have anti-diabetic and anti-obesity activity. Synthetic accessibility of the molecule is also found to be of good potential. Further invitro and in vivo investigation is necessary for the assigning these novel molecules as anti-diabetic and anti-obesity treatment strategy.

#### References:

1. Subauste, A., & Burant, C. F. (2003). DGAT: novel therapeutic target for obesity and type 2 diabetes mellitus. *Current Drug Targets-Immune, Endocrine & Metabolic Disorders*, 3(4), 263-270.
2. Subauste A, Burant CF. Dgat: novel therapeutic target for obesity and type 2 diabetes mellitus. *Curr Drug Targets Immune Endocr Metabol Disord* 2003; 3:263–70.3.
3. Capeau J. Insulin resistance and steatosis in humans. *Diabetes Metab* 2008;34:649–57.

4. Erion, D. M., Park, H. J., & Lee, H. Y. (2016). The role of lipids in the pathogenesis and treatment of type 2 diabetes and associated co-morbidities. *BMB reports*, 49(3), 139.
5. Wajchenberg BL (2007) beta-cell failure in diabetes and preservation by clinical treatment. *Endocr Rev* 28, 187-218
6. Rothman DL, Shulman RG and Shulman GI (1992) <sup>31</sup>P nuclear magnetic resonance measurements of muscle glucose-6-phosphate. Evidence for reduced insulin-dependent muscle glucose transport or phosphorylation activity in non-insulin-dependent diabetes mellitus. *J Clin Invest* 89, 1069-1075
7. Shulman GI, Rothman DL, Jue T, Stein P, DeFronzo RA and Shulman RG (1990) Quantitation of muscle glycogen synthesis in normal subjects and subjects with non-insulin-dependent diabetes by <sup>13</sup>C nuclear magnetic resonance spectroscopy. *N Engl J Med* 322, 223-228
8. Hwang JH, Perseghin G, Rothman DL et al (1995) Impaired net hepatic glycogen synthesis in insulin-dependent diabetic subjects during mixed meal ingestion. A <sup>13</sup>C nuclear magnetic resonance spectroscopy study. *J Clin Invest* 95, 783-787
9. Landau BR, Wahren J, Chandramouli V, Schumann WC, Ekberg K and Kalhan SC (1996) Contributions of gluconeogenesis to glucose production in the fasted state. *J Clin Invest* 98, 378-385
10. Tsuda, N., Kumadaki, S., Higashi, C., Ozawa, M., Shinozaki, M., Kato, Y., ... & Furusako, S. (2014). Intestine-targeted DGAT1 inhibition improves obesity and insulin resistance without skin aberrations in mice. *PLoS One*, 9(11), e112027.
11. Denison, H. et al. Diacylglycerol acyltransferase 1 inhibition with AZD7687 alters lipid handling and hormone secretion in the gut with intolerable side effects: a randomized clinical trial. *Diabetes Obes. Metab.* 16, 334–343 (2014).
12. Haas, J. T. et al. DGAT1 mutation is linked to a congenital diarrheal disorder. *J. Clin. Invest.* 122, 4680–4684 (2012)
13. McCoull W, Addie MS, Birch AM, et al. Identification, optimization and in vivo evaluation of oxadiazole dgat-1 inhibitors for the treatment of obesity and diabetes. *Bioorg MedChem Lett* 2012; 22:3873–8.13.
14. Meyers C, Gaudet D, Tremblay K, et al. The dgat1 inhibitor lrcq908 decreases triglyceride levels in patients with the familial chylomicronemia syndrome. *J Clin Lipidol* 2012; 6:266–7.14.
15. King AJ, Segreti JA, Larson KJ, et al. Diacylglycerol acyltransferase 1 inhibition lowers serum triglycerides in the Zucker fatty rat and the hyperlipidemic hamster. *J Pharmacol Exp Ther* 2009; 330:526–31.
16. Zhao G, Souers AJ, Voorbach M, et al. Validation of diacylglycerol acyltransferase 1 as a novel target for the treatment of obesity and dyslipidemia using a potent and selective small molecule inhibitor. *J Med Chem* 2008; 51:380–3.
17. Qian Y, Wertheimer SJ, Ahmad M, et al. Discovery of orally active carboxylic acid derivatives of 2-phenyl-5-trifluoromethyl-oxazole-4-carboxamide as potent diacylglycerol acyltransferase-1 inhibitors for the potential treatment of obesity and diabetes. *J Med Chem* 2011; 54:2433–46
18. Oldendorf WH, Measurement of brain uptake of radiolabeled substances using a tritiated water internal standard, *Brain Res*, 1970; 24(2):372-376.
19. Daina, A., Michielin, O., & Zoete, V. (2017). SwissADME: a free web tool to evaluate pharmacokinetics, drug-likeness and medicinal chemistry friendliness of small molecules. *Scientific reports*, 7(1), 42717.
20. Daina, A., & Zoete, V. (2016). A boiled-egg to predict gastrointestinal absorption and brain penetration of small molecules. *ChemMedChem*, 11(11), 1117-1121.

21. Pires, D. E., Blundell, T. L., & Ascher, D. B. (2015). pkCSM: predicting small-molecule pharmacokinetic and toxicity properties using graph-based signatures. *Journal of medicinal chemistry*, 58(9), 4066-4072.
22. Filimonov D. A. et al., "Prediction of the Biological Activity Spectra of Organic Compounds Using the Pass Online Web Resource," *Chem. Heterocycl. Compd.*, vol. 50, no. 3, pp. 444–457, 2014. <https://doi.org/10.1007/s10593-014-1496->